Mechanics of Advanced Composite Structures

Journal homepage: https://macs.semnan.ac.ir/

Semnan University

ISSN: 2423-7043

Research Article

Influence of Plate Thickness and Mineral Admixtures on Flexural Behaviour of RC Slab – An Experimental Investigation.

Reena Kotresh*, Eramma Hanumanthappa

Department of Studies in Civil Engineering, UBDT College of Engineering, Davanagere-577004, Karnataka, India.

ARTICLE INFO

Article history:

Received: 2023-10-19
Revised: 2024-03-22
Accepted: 2024-05-12

Keywords:

Ground-Granulated Blast Furnace Slag;
Nano Silica;
Optimum Dosage;
High-density concrete;
Scanning electron microscopy.

ABSTRACT

This study is focused on evaluating the behaviour of use of alternatives for cement, namely, Ground-Granulated Blast Furnace Slag (GGBS) and Nano Silica (NS), on the mechanical, microstructure, and structural behavior of reinforced concrete (RC) slabs. Concrete was made with various dosages of GGBS from 0% to 50% at a rate of 5% and NS dosage from 0.1% to 1% at an interval of 0.1%. Compressive and tensile strength of concrete was evaluated along with microstructural characteristics using Scanning Electron Microscopy (SEM). The optimum dosages were found to be 10% GGBS and 0.3% NS by cement weight. This optimum dosage was used in making RC slabs with dimensions 1200 x 1200 x 100 mm, varying the slab thickness. To determine the stiffness and load-bearing capacity of the slabs, two-point loading was applied. Use of GGBS and NS results in high-density and high-strength concrete. Such research works highlight the prospective use of GGBS and NS in sustainable construction, encouraging cost-effective, eco-friendly practices with innovations in concrete technology.

1. Introduction

Concrete remains the most widely used construction material in the world, and this shows how much it plays a critical role in the development of modern infrastructure. Estimated at 2.8 billion tons in 2015, that is roughly 1.5 cubic meters per person, it underlines its indispensable use in contemporary construction [1-2]. However, there is a substantial environmental cost associated with this ubiquity. The main binder in concrete, cement, contributes significantly to carbon dioxide emissions worldwide, making up over 6% of the total. 1.25 tonnes of carbon dioxide are discharged into the atmosphere for every tonne of cement produced. These emissions mainly come from two key processes: the decarbonation of limestone, which accounts for 60–65% of the emissions, and the high energy input to heat the cement kiln, which accounts for the remaining 35–40% [3-4]. With the rapid pace of global development, cement demand is expected to increase significantly, possibly to an alarming 18 billion tons per year by 2050 [5].

This expected increase in demand is posing significant environmental problems and is forcing the construction industry to find

* **Corresponding author.**
E-mail address: reena.andnur@gmail.com

Cite this article as:

solutions for sustainable development. The reduction of cement consumption by introducing alternative materials is one of the most promising ways of decreasing the carbon footprint of concrete. Fly ash, bagasse ash, ground granulated blast furnace slag (GGBS), and silica fume are supplementary cementitious materials that are investigated by material scientists and researchers. Besides being carbon emission mitigation measures during cement production, these supplementary cementitious materials provide performance advantages to concrete: improved strength, durability, and workability [6].

Among these alternatives, GGBS has gained a lot of attention due to its favorable properties and due to its status as an industrial by-product. GGBS is produced through the blast furnace process of manufacturing steel. This involves blending iron ore, limestone, and coke in temperatures ranging between 1400°C and 1500°C. This eventually yields liquid slag, separated with the rapid cooling by water of the iron particles it carries. The remaining one consists of silicates, aluminates, and calcium oxides. Then it is ground into fine powder to become GGBS [7]. GGBS includes concrete that significantly enhances its performance mechanically, is abrasion-resistant, and durable for a very long time. Moreover, it reduces the embodied carbon of material used in concrete, as well as helps this industry meet the sustainability goals they set for themselves [1].

However, GGBS has several drawbacks, especially in terms of early-age strength development. The property makes GGBS less suitable for applications that need high initial compressive strength, such as precast concrete manufacturing or situations requiring rapid removal of formwork. These limitations call for further research into ways of optimizing the performance of GGBS in early strength applications or the creation of supplementary materials to fill the gaps. [8].

Parallel with all these developments, the innovation in nanotechnology has been creating new scopes for improvement and sustainability of concrete. Among different kinds of nanomaterials, NS has proved itself as the most promising additive that transforms conventional concrete into a very high-strength, sustainable, and environmentally friendly product. Nano-silica contains silica particles that are nano-scaled and have unusual characteristics that promote both mechanical properties and durability of the concrete. Because of superfine particle size and an associated high surface area, this material proves to be efficient as a filler capable of optimizing the binder paste microstructure. Consequently, the improvement of the nano-structure significantly improves the long-term performance of concrete by lowering cement consumption and also diminishing its carbon footprint [9], [10], [11], [12].

The main manner by which Nano-silica exercises its effect on concrete is by acting as a pozzolanic material. Nano-silica reacts with calcium hydroxide (CH) that results as a by-product from the hydration of cement, producing calcium silicate hydrate (C-S-H). It is the compound through which strength and durability, for the most part, are provided. This pozzolanic reaction not only improves the mechanical properties of concrete but also decreases the permeability of the product, thereby enhancing its strength against environmental degradation [13]. Nano-silica also assists in reducing segregation and bleeding of the freshly mixed concrete, in providing extended setting times, and in improving the cohesiveness of the mixture. The properties of nano-silica make it of great value for concrete formulation, especially when applications require high-performance materials.

Moreover, Nano-silica promotes the early hydration process of cement by enhancing the rate of dissolution of tricalcium silicate for the rapid formation of C-S-H gel. Thus, this mechanism is able to enhance not only early strength development but also the overall durability of hardened concrete. Advanced microscopic techniques, including TEM, have unravelled the fine structure of Nano-silica and its efficiency as a filler material in concrete, further confirming its promising role as a high-performance additive [14], [15].

Although the benefits of GGBS and Nano-silica are many, there are challenges as well as knowledge gaps. In that context, even though Nano-silica exhibits superior performance in developing the mechanical and durability characteristics of concrete, its application in concrete mixes is extremely expensive and involves complex handling for uniform dispersion. Moreover, the performance optimization and sustainability of the GGBS-Nano-silica concrete system have received inadequate attention. The main implication of this is a strong need for comprehensive research that allows one to understand the synergistic interaction between these materials in a way that enables optimizing the mix design with maximum benefit from their complementary properties.

This work aims to fill the gap by systematically evaluating the use of GGBS and Nano-silica in concrete. Herein, the study will assess the impact of GGBS and NS on the mechanical properties of the concrete. The research explores developing a concrete that provides outstanding performance but minimizes the carbon footprint associated with

construction materials. The work is expected to form part of the larger efforts geared toward advancing sustainable construction practices in order to reduce degradation of the environment, an action that is supported by the efforts of the entire globe toward mitigating climate change. Through rigorous experimentation and analysis, the findings of this study are expected to provide valuable insights into the potential of GGBS and Nano-silica as key components in the next generation of sustainable construction materials.

Recent analytical and numerical models on advanced sandwich and composite shells highlight the significance of structural configuration in enhancing vibroacoustic and mechanical performance [26–28]. These studies emphasize how core geometry, material choice, and curvature influence stiffness, ductility, and sound insulation. Drawing from such insights, the present work explores the role of plate thickness and mineral admixtures in improving the flexural behavior of RC slabs. This experimental approach bridges material innovations with structural efficiency for sustainable construction practice.

Recent fracture and delamination studies emphasize the role of material composition, geometry, and process zone effects in improving structural strength and resistance [29–32]. These works demonstrate how advanced modeling approaches capture fracture toughness and crack propagation with greater accuracy. Drawing from such insights, the present study investigates how plate thickness and mineral admixtures influence the flexural response of RC slabs. This experimental analysis links material optimization with enhanced structural performance for sustainable construction.

2. Materials and Methodology

The methodology adopted for this investigation is systematically designed to estimate the mechanical properties of GGBS-NS replacement cement concrete. It analyzes the optimal percentages of incorporation of GGBS and NS, which can provide sustainable cementitious materials, leading towards a better durability of structures while enhancing their strength to some extent. FRP-reinforced slab studies [33] highlight how reinforcement type and surface properties affect flexural response, aligning with the present work on plate thickness and mineral admixtures in enhancing RC slab performance. The process involves careful selection and testing of materials, concrete mix design, specimen preparation, and mechanical property evaluation. This current study intends to provide a simple solution for the utilization of secondary cementitious materials to explore the enhancement of the mechanical performance of cementitious composites. In this regard, a conventional mixing approach was employed. The materials utilized in this investigation include ordinary Portland cement (OPC) of grade 53, manufactured sand (M-sand) as fine aggregate, and crushed granite ballast of size 20–12.5 mm as coarse aggregate. The GGBS and NS were procured from local vendors to ensure consistency in quality and availability. A commercially available superplasticizer, FOSROC SP430DIS, was incorporated into the mix to achieve the desired workability and water reduction without compromising strength. The water-cement ratio and superplasticizer were maintained at 0.45 and 0.3, respectively. Additionally, reinforcing steel bars FE 550 with a yield strength of 550 MPa were used for slab casting and testing. The physical and chemical properties of all materials were carefully determined following standard testing protocols and are summarized in Table 1. The mix design for M30 grade concrete was developed in accordance with the Indian Standard IS 10262:2019 guidelines. To systematically investigate the influence of GGBS and NS on concrete properties, cement was partially replaced by GGBS in varying proportions, ranging from 0% to 50% in 5% increments. Similarly, NS was introduced into the concrete mix in incremental levels ranging from 0.1% to 1%, with an interval of 0.1%. This stepwise approach ensured a comprehensive evaluation of their effects on concrete strength characteristics. Concrete specimens were cast for each mix variation to determine both compressive and split tensile strengths. Cylindrical specimens of standard dimensions (150 mm × 300 mm) were prepared for each combination of GGBS and NS, including mixes containing both materials simultaneously. The batching of concrete was carried out using a conventional drum mixer as per IS 1791 (1985). The concrete specimens were demolded after 24 hours and subjected to curing in water for 28 days under controlled conditions. Subsequently, compressive strength and split tensile strength tests were conducted following the procedures outlined in IS 516:1959 and IS 5816:1999, respectively.

Table 1. Properties of Materials.

Sl no	Material	Test	Result	Codes
1	C	G IST FST NC Fineness	3.14 95min 172min 30 % 6%	IS 4031-11 (1980) IS4031 (Part-5)-2019
2	FA	G Zone WA	2.6 II 1.2%	IS 2386: 1963(Part 3)
3	CA	G WA	2.6 1.2%	IS 2386: 1963 (Part 3)
4	GGBS	G	2.86	IS 16714 – 2018
5	NS	G	1.1	IS 15388-2003
6	SP	G	1.2	
7	Steel	σ_y	551.2	IS 1608 - 2018

Note:
G – Specific gravity,
IST – Initial setting time,
FST – final setting statement,
NC – Normal consistency,
WA – Water absorption,
σ_y – yield strength, MPa.

Based on the results, it was observed that the optimal compressive and Split tensile strength were achieved at a 10% replacement of cement with GGBS and 0.3% incorporation of nano-silica. To validate these findings on a structural scale, concrete slabs with the optimum combination of GGBS and NS were cast with the mix proportions as indicated in Table 2. The slabs had dimensions of 1200 × 1200 × 100 mm as shown in Figure 1, and were reinforced with steel bars to ensure realistic structural behavior. The casting process was carried out to ensure uniform distribution of material and compaction. Two-point loading conditions were applied to the slabs to study their flexural behavior and ultimate load-carrying capacity. The two-point loading test setup is shown in Figure 2 (a,b). It is a representation of the support arrangement and application of load. Load was gradually applied until failure using a hydraulic jack, and all-important critical parameters such as the behavior of load-deflection cracking pattern, and the ultimate capacity in load were captured. Testing enabled concrete reinforced with GGBS and NS performance insights into structural conditions that aided the identification of the best combinations that are effective in obtaining good strength and durability.

Table 2 Mix proportion

Sl. No	Mix type	C	NS	GGBS	FA	CA
1	CM	421.21	0	0	961.3	865.2
2	O_G	391.96	0	29.24	961.3	865.2
3	O_{NS}	419.94	1.26	0	961.3	865.2
4	O_{GNS}	341.76	1.26	29.24	927.3	827.7

Note:
CM- Control mix,
O_G - Optimum mix(GGBS),
O_N - Optimum mix (NS),
O_{NG} - Optimum mix (GGBS+NS)
C – Cement Kg/m³,
NS - Nano silica Kg/m³,
GGBS - Kg/m³,
FA – Fine Aggregate Kg/m³,
CA – Coarse aggregate Kg/m³.

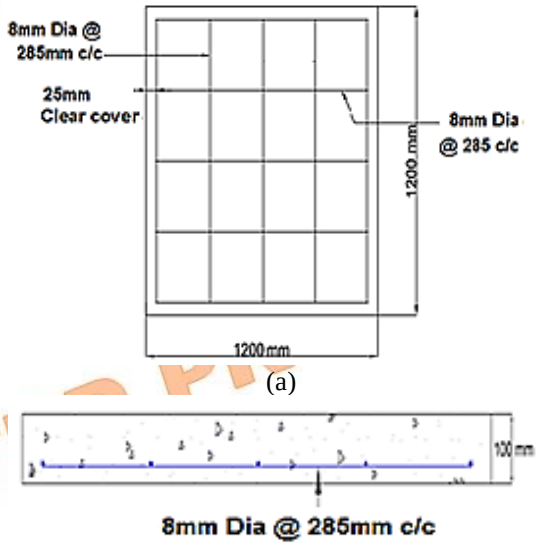

(a)

(b)

Fig. 1. Plan and Section of the slab

(a)

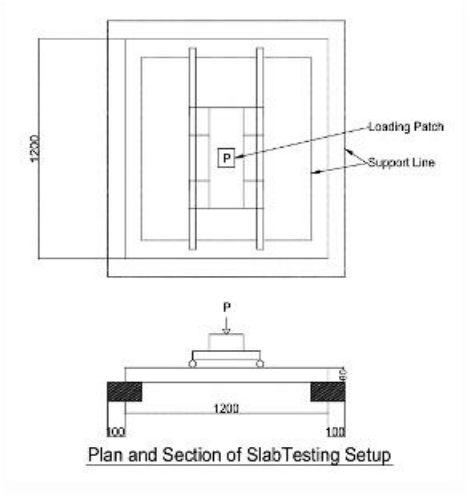

(b)

Fig 2. Two Point Loading Setup

3. Results and Discussion

3.1. Hardened Properties: Compressive Strength

Figure 3 demonstrates the variation in compressive strength of concrete at 7 days and 28 days for different percentages of GGBS ranging from 0% to 50%. The compressive strength increases with GGBS addition, but after reaching a certain level, it again decreases with higher substitution percentages. At 10% substitution of GGBS, the compressive strength peaks at 28 days at 41.53 MPa, which presents an 18.2% improvement compared to the control mix of 35.12 MPa. Similar trends were observed at 7 days, where it increased to 29.31 MPa. Here, it also presents a 13.4% improvement compared to the control mix of 25.85 MPa. Beyond 10% replacement, the strength degrades in a continuous manner. At 50% GGBS replacement, the strength at 28 days decreased to 22.57 MPa, which is 35.7% lower than that of the control. This trend shows that GGBS can improve strength through pozzolanic reaction by forming calcium silicate hydrate (C-S-H) gel, which increases long-term strength and durability. However, higher GGBS content dilutes cementitious material, causing strength loss, especially at early curing stages, due to its slower hydration. The outcomes are in agreement with those reported by Gopalakrishnan et al. [16], who found strength improvement with GGBS up to 15% replacement but reported strength decline beyond this percentage due to delayed hydration. Similarly, Saha [17] pointed out that although GGBS enhances durability, its slow pozzolanic reaction retards early-age strength gain.

The compressive strength variations with NS content between 0% and 1% is shown in Figure 4. Peak values for both 7-day and 28-day strengths occur at 0.3% NS content. Compressive strength at 28 days is 43.43 MPa, representing a 23.7% gain from the control mix of 35.12 MPa. The strength also increases at 7 days to 32.14 MPa, that is, by 24.3% compared with the control. This is due to high pozzolanic reactivity and filler effects of NS. Nano-silica particles fill microvoids and react with calcium hydroxide to form additional C-S-H gel, improving early and long-term strength significantly. Beyond 0.3% NS, compressive strength starts to decrease; for example, at 1% NS, the 28-day strength decreases to 25.6 MPa. This must be attributed to the aggregation of NS particles at higher dosage levels, which leads to weaker zones and lower hydration efficiencies. The results are comparable with the study of Singh and Siddique [18], wherein they have reported optimal strengths at 0.3% NS and have identified diminishing returns beyond this point. Similarly, Torkittikul et al. [19] showed that excessive NS content causes particle clustering and leads to a reduction in the concrete's strength enhancement potential.

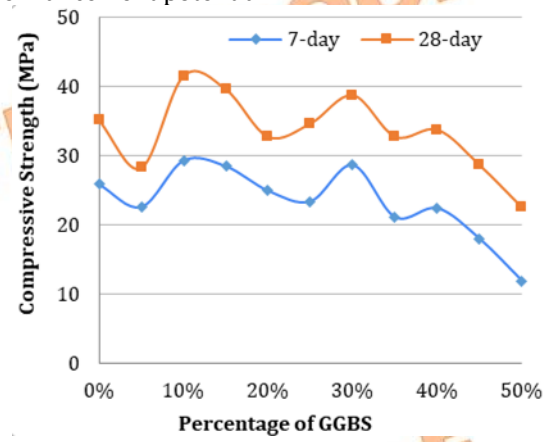

Fig. 3. Determination of optimum dosage of Compressive strength of GGBS

The compressive strength comparison for the four cases presented in Figure 5 is for the control mix, 10% GGBS, 0.3% NS, and the combined mix of 10% GGBS + 0.3% NS. The outcome suggests that concrete compressive strength improves in both cases for GGBS and NS separately. The 28-day strength of 10% GGBS is about 41.53 MPa with an increase of 18.2% over control, and of 0.3% NS about 43.43 MPa with an increment of 23.7%.

However, the combined mix of 10% GGBS and 0.3% NS results in a compressive strength of 38.97 MPa at 28 days, showing a 10.5% improvement over the control mix but a slight reduction compared to their individual optimal strengths. The combined effect indicates that while GGBS and NS complement each other's pozzolanic activity, their simultaneous use may slightly hinder hydration kinetics due to particle

interactions or competition for available calcium hydroxide.

Figure 6 shows the trend in compressive strength variation as a function of cement content. The strength-to-cement ratio follows a gradual decline with an increase in cement content, having a slope of -0.7999 and an R^2 value of 0.5805, which represents moderate correlation. This curve clearly shows that the rate of return in strength is declining with an increase in the dosage of cement. Higher cement content mainly enhances the compressive strength; however, it cannot contribute proportionally when the amounts are high due to inefficient hydration in such high-cement-content compositions, which can generate more heat and produce micro-cracks.

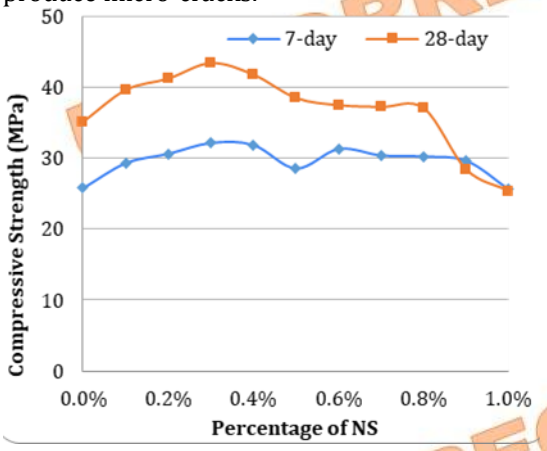

Fig. 4. Determination of optimum dosage of Compressive strength of Nano-Silica

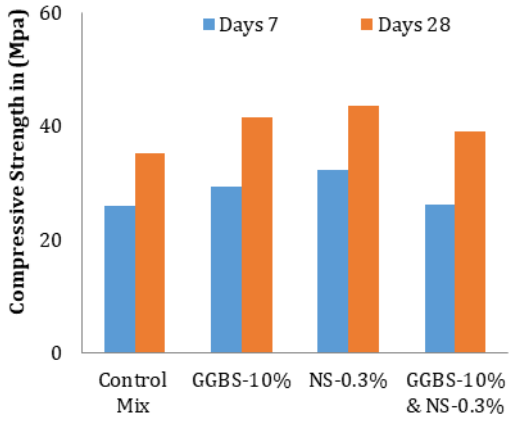

Fig.5. Compression Strength of GGBS+NS

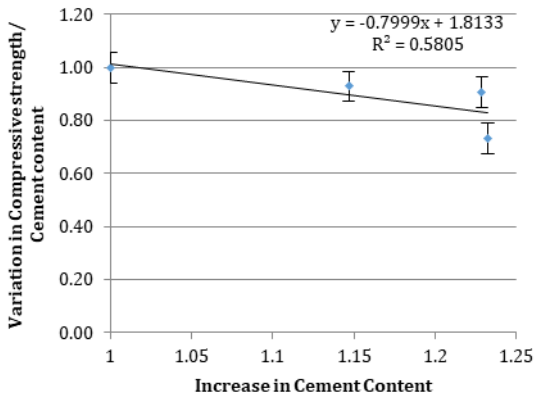

Fig. 6. Variation of Compressive strength due to reduction in Cement content

3.2. Split Tensile Strength

Split tensile strength of the concrete at 28 days for four different conditions: control mix, 10% GGBS, 0.3% NS, and the combined mix of 10% GGBS along with 0.3% NS are represented in Table 3 and Figure 7, respectively. An essential characteristic to understand the tensile behavior of concrete is split tensile strength, which is directly related to the endurance and structural integrity of concrete components. The split tensile strength of the control mix at 28 days is 3.41 MPa, which serves as the baseline for comparison.

The tensile strength increased significantly with 10% GGBS as a partial replacement for cement to 4.51 MPa, representing an improvement of 32.3% over the control mix. This improvement can be attributed to the pozzolanic reactivity of GGBS, enhancing the microstructure of concrete through the production of extra C-S-H gel. Such a reaction reduces voids and improves tensile properties, thus enhancing concrete performance. Similarly, with 0.3% NS, tensile strength is 4.16 MPa, an increase of 22% as compared to the control mix. The improvement in NS is due to nanoscale particle size along with an increase in cementitious matrix density brought about by filler effects and hydration acceleration. Moreover, nano-silica acts as a nucleation site for hydration products, thus helping to densify the concrete structure. Since NS primarily promotes early hydration rather than enhancing long-term tensile strength, the improvement in tensile strength with NS is marginally smaller than that of GGBS.

The highest split tensile strength of 4.87 MPa is obtained at the mixed proportion of 10% GGBS and 0.3% NS, which provides a strength improvement of about 42.8% over the control mix. This will indicate the synergistic action by NS interacting with GGBS so as to accelerate the hydration process, and that GGBS contributes

significantly to long-term strength gained mainly via the pozzolanic reactivity. Together, they enhance split tensile properties, reduce porosity, and improve the microstructure. However, the strength added would be somewhat lesser than what is theoretically considered as a sum of individual contributions from GGBS and NS because GGBS and NS do compete with each other in terms of usage of the calcium hydroxide, thus slightly reducing the overall hydration efficiency.

The outcomes indicated a consistent improvement in the split tensile strength by the addition of GGBS, NS, and their combination. GGBS improved the split tensile strength through chemical reaction with calcium hydroxide (CH), the cement hydration by-product, in producing supplementary C-S-H gel to increase the ITZ strength between the aggregate surface and the cement paste. Pozzolanic reaction also occurs, but at a slower rate; hence, significant long-term strength improvement occurs as well. On the contrary, Nano-Silica fills microvoids through nanoscale particles and enhances tensile strength by densifying the cementitious matrix. The NS also accelerates hydration in tricalcium silicate (C3S), forming more C-S-H gel at early stages, thus contributing to early strength gains.

The combined mixture of GGBS and NS surpasses their individual usages, which suggests that their interaction improves both the early-age and long-term strength properties. These are in agreement with earlier work [20, 21, 22]. Overall, the results prove that supplementary cementitious materials such as GGBS and Nano-Silica are effective in enhancing the tensile strength of concrete while also promoting sustainability.

Table 3: Split tensile strength in MPa

Sl no	Mix type	Average split tensile strength at 28days in MPa
1	Control mix	3.41
2	GGBS (10%)	4.51
3	NS (0.3%)	4.16
4	GGBS (10%)+NS(0.3%)	4.87

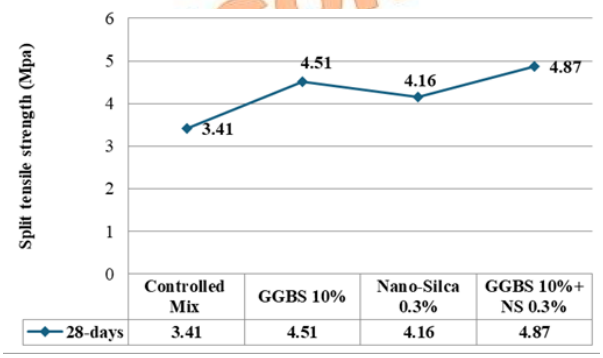

Fig. 7. Comparison of Split tensile strength.

This variation in strength characteristic of concrete was influenced by the density of the concrete mix. The density of concrete increased by around 5% when the GGBS and NS dosage was up to 20% and 0.7%, respectively.

3.3. Modulus of Elasticity

Figure 8 indicates the compressive loading stress-strain behavior of concrete for the mixes of control mix (CC), 0.3% Nano-Silica (NS), 10% Ground Granulated Blast Furnace Slag (GGBS), and the combination of 10% GGBS and 0.3% NS, and are tabulated in Table 4. The trend depicted in the graph shows substantial improvements in the modulus of elasticity of concrete with GGBS and NS when compared to the control mix. The stress-strain curve for the control mix CC is nearly linear with a moderate slope, which shows a low modulus of elasticity. The equation for the control mix is y=111,835.54x+11, 408.53y = 111,835.54x + 11, 408.53y =111,835.54x+11,408.53, and the curve follows a steady increase in stress with increasing strain. Incorporating 0.3% NS improves the slope of the stress-strain curve, as seen in the equation 1.

$$y = -8{,}303{,}011.13x^2 + 26{,}509.84xy = -8{,}303{,}011.13x^2 + 26{,}509.84xy = -8{,}303{,}011.13x^2 + 26{,}509.84x \quad (1)$$

The curve indicates more significant stress resistance for the same amount of strain as against the control mix, indicating an increase in modulus of elasticity. This improvement has its origin in Nano-Silica's capability of further refining the microstructure of concrete through the filling of voids, along with accelerating the hydration process, resulting in a denser matrix of cement. This improvement in elastic modulus for the NS mix means a 23.3% increase as compared to the control mix. Therefore, this is a great indication of material efficacy in increasing stiffness.
The GGBS mix with 10% shows more stiffness, and this is indicated by the equation 2.

$$y = -7{,}804{,}876.70x^2 + 28{,}673.79xy = -7{,}804{,}876.70x^2 + 28{,}673.79xy = -7{,}804{,}876.70x^2 + 28{,}673.79x. \quad (2)$$

The slope of this curve exceeds both the control and the NS mix, which indicates the modulus of elasticity has increased significantly. This is due to the pozzolanic reaction of GGBS, contributing to the creation of additional calcium silicate hydrate gel, thus reducing microvoids and improving stiffness. For the GGBS mix, its

modulus of elasticity improves by almost 29.5% compared to the control mix.
The combined mix of 10% GGBS and 0.3% NS is one having the steepest slope as well as the highest modulus of elasticity, as calculated from equation 3

$$y = -9{,}600{,}899.72x^2 + 24{,}734.13xy$$

$$= -9{,}600{,}899.72x^2 + 24{,}734.13xy$$
$$= -9{,}600{,}899.72x^2 + 24{,}734.13xy \quad (3)$$

This synergistic blend results in superior deformation resistance, achieving a 38.7% modulus of elasticity increment over the control mix. The combined effect is attributed to the simultaneous benefits of GGBS and NS, which enhance early-age hydration and microstructure refinement due to the addition of Nano-Silica and provide long-term pozzolanic activity due to GGBS, giving rise to a dense and resilient cementitious matrix. All curves show good coefficient of determination values between 0.96 and 1.0, suggesting excellent precision and reliability of the data gathered in experiments.
Overall, the trend confirms that both GGBS and Nano-Silica are able to enhance the stiffness of concrete, with the best result being obtained when GGBS and Nano-Silica are used together. Therefore, the outcomes reveal that the addition of optimum dosages of GGBS and Nano-Silica improves the modulus of elasticity, and the concrete mix will be less deformable. The results obtained have practical implications in structural applications where high stiffness and low deflection are required.

Table 4: Young's Modulus of different combinations

Sl no	Mix	Average modulus of Elasticity at 28 days in GPa
1	Control	11.408
2	10% GGBS	28.673
3	0.3% NS	26.509
4	GGBS+NS	24.734

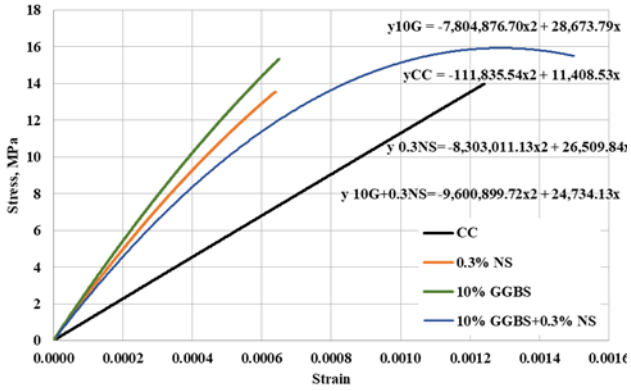

Fig. 8. Youngs Modulus of Conventional Concrete, GGBS, NS, GGBS+NS

3.4. Load Deflection Curve and Ductility Index

An assessment of the load-deflection behavior and ductility characteristics of concrete slabs made with GGBS, Nano-Silica (NS), and a combination of both was made at different aggregate sizes and slab thicknesses. The performance varies extensively, depending on the composition of the material and structural parameters, as indicated in the load-deflection curves and tabulated values. Different slab configurations were investigated to obtain maximum load-carrying capacity, central deflection, and ductility index. Control mix yielded peak load 103.22 kN at a central deflection of 4.8 mm, resulting in a ductility index, β, of 4.36, which was considered the baseline.

In 10% GGBS reinforced slabs, load carrying capacity increased up to 148.76 kN, along with reducing the deflection up to 3.48 mm, with an enhancement in ductility index at 4.83. Improvement is seen up to around 44% with an increase in load carrying capacity compared with control specimens because of the pozzolanic reactivity of GGBS, and enhancing the stiffness with improvement in load resistance [20-21]. Similarly, a peak load of 152.00 kN and a deflection of 7.99 mm were obtained with the addition of 0.3% NS, attaining a ductility index of 6.00, which is 47.2% better than that of the control. The superiority in ductility achieved with the use of NS is on account of its filler effect along with microstructural refinement that would enhance the toughness of concrete [22-23].

The combination of 10% GGBS and 0.3% NS with aggregate sizes of 20–12.5 mm exhibited a peak load of 185.13 kN and a deflection of 25.24 mm, yielding a ductility index of 5.59. This combination demonstrated a remarkable 79.4% increase in load capacity compared to the control, highlighting the synergistic effect of GGBS and NS in enhancing the load-bearing capacity and ductility of the concrete. For the same combination with aggregate sizes of 12.5–10 mm, the peak load was slightly lower at 151.75 kN,

with a deflection of 20.06 mm and a ductility index of 5.93. The higher ductility in this case, compared to the larger aggregate size, suggests that finer aggregates contribute to better crack control and load distribution.

Distinct trends were observed in the varying thickness slabs. The slab with 80 mm exhibited a peak load of 154.91 kN and 42.71 mm of deflection and a ductility index of 3.87. The lower capacity of load was noted for the slabs that have a thickness of 60 mm and 40 mm, 42.00 kN and 24.30 kN, respectively. Highly increased deflections with corresponding high values of ductility index 7.23 and 8.5 were noticed. These results demonstrate that thinner slabs exhibit higher ductility due to their increased flexibility, but at the cost of reduced load-bearing capacity. The load-deflection curve was plotted as indicated in Figures 9 and 10. The Ductility Index (β) gives information about the ability of the reinforcing material to provide ductility to the structural elements. The ductility index for structural components is in the range of 4 to 6. Based on the data in the table shown in Table 5, a specimen of slab with a GGBS+NS combination of 12.5mm-10mm aggregate presents more ductility than others [22].

Table 5: Flexure test results.

Sl no.	Slab specimen	Pfc (kN)	δfc (mm)	PU (kN)	δU (mm)	β= δU/ δfc
1.	Control Mix (100mm Thick)	154.6	1.10	103.22	4.8	4.36
2.	GGBS (10%) (100mm Thick)	57.68	0.72	148.76	3.48	4.83
3.	NS (0.3%) (100mm Thick)	72.86	1.33	152.00	7.99	6.00
4.	GGBS+NS (20-12.5mm) (100mm Thick)	63.83	3.83	185.13	25.24	5.59
5.	GGBS+NS (12.5-10mm) (100mm Thick)	84.98	3.38	151.75	20.06	5.93
6.	GGBS+NS (80 mm thick slab)	106.31	11.01	154.91	42.71	3.87
7.	GGBS+NS (60 mm thick slab)	16.00	1.81	42.00	13.1	7.23
8.	GGBS+NS (40 mm thick slab)	12.15	3.54	24.30	30.1	8.5

where
Pfc = Load at first crack
δfc= Deflection at first crack
PU = Load at failure
δU= Defelction at failure
β= Ductility index

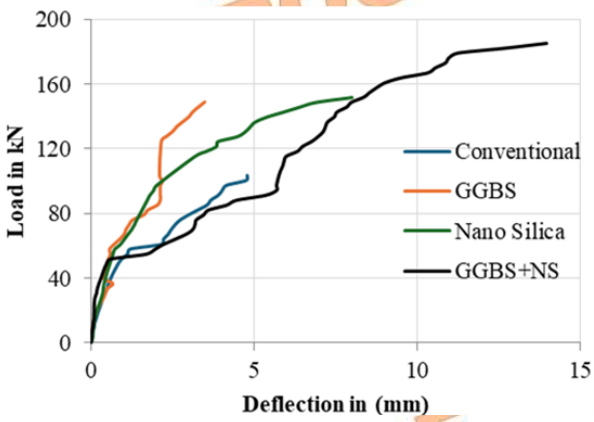

Fig. 9. Variation of load and deflection of slabs of different combinations

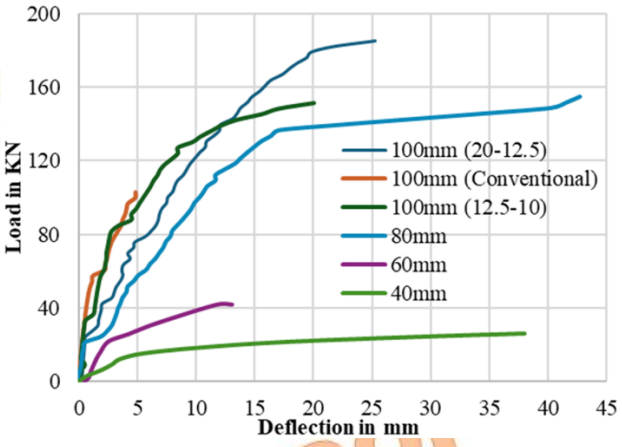

Fig. 10. Variation of load and deflection of slabs of different thickness with 10%GGBS+0.3% NS

3.5. Stiffness

The slab specimen's stiffness was determined based on the ratio of load at the first crack and corresponding deformation, which estimates the initial resistance to deformation before a considerable amount of cracking. The obtained results are shown in Table 6; the control mix with a thickness of 100 mm has a stiffness equal to 54.64 kN/mm. When GGBS was incorporated at 10% replacement, with a slab thickness of 100 mm, stiffness increased to 139.65 kN/mm and thus showed a significant increase in resistance to deformation as a result of the pozzolanic properties of GGBS. In comparison, the inclusion of nano-silica (NS) at 0.3% resulted in a moderate increase in stiffness to 63.75 kN/mm. However, when GGBS and NS were combined with varying

aggregate sizes, such as 20–12.5 mm and 12.5–10 mm, the stiffness dropped to 51.59 kN/mm and 51.63 kN/mm, respectively, indicating a complex interaction between the aggregate grading and the modified binder matrix.

Notably, the values of stiffness dropped drastically in thinner slab specimens, and even in the combinations of GGBS+NS, it showed 24.30 kN/mm at a thickness of 80 mm, while 9.11 kN/mm at 60 mm, and just 4.16 kN/mm at 40 mm. This trend indicates a significant influence of thickness on stiffness, as thinner slabs have a reduced capacity to resist deformation. Moreover, GGBS+NS with 12.5 mm down-passing aggregate was found to have the highest stiffness compared to other proportions, indicating optimization of the size of aggregate for improved load distribution and matrix reinforcement.

The percentage increase in stiffness for GGBS (10%) over the control mix is approximately 155.5%, while NS (0.3%) leads to a 16.7% improvement. The stiffness reduction for GGBS+NS combinations compared to the control mix ranges from 5.6% to 7.6% for the 12.5–10 mm aggregate gradation. The stiffness decline due to reduced slab thickness is pronounced, with reductions of 55.5%, 83.3%, and 92.4% for 80 mm, 60 mm, and 40 mm slabs, respectively, compared to the 100 mm thickness.

Table 6: Stiffness of slab of different combinations

Slab specimen	Stiffness (KN/mm)
Control mix (100mm)	54.64
GGBS (10% & 100mm)	139.65
NS (0.3% & 100mm)	63.75
GGBS+NS (20-12.5 &12.5-10mm) (100mm)	51.59
GGBS+NS (12.5-10mm) (100mm)	51.63
GGBS+NS (80mm)	24.30
GGBS+NS (60mm)	9.11
GGBS+NS (40mm)	4.16

3.6. X-RAY Diffraction (XRD)

XRD analysis presented in Figure 11 of concretes incorporating GGBS and NS provides notable information regarding the material's microscopic composition. The diffraction patterns indicate the presence of crucial phases and elements, such as the presence of calcium, silicon, and aluminum, associated with the formation of essential strength- and durability-enhancing compounds like Calcium Silicate Hydrate and ettringite. The peaks corresponding to these phases indicate their abundant formation, particularly in mixes containing NS and GGBS.

It is clear that the addition of nano-silica affects the production of C-S-H, as seen from the enhanced peaks associated with this phase in the XRD patterns. The pozzolanic reactivity of Nano-Silica and its nanoscale particle size, which offers more nucleation sites for hydration products, are responsible for this improvement. The increased formation of C-S-H results in a denser and more refined cementitious matrix, greatly enhancing the mechanical qualities and permeability resistance of the concrete.

At the same time, GGBS affects the microstructure by lessening the calcium hydroxide peaks' intensity, which shows that there is less free calcium hydroxide in the matrix. The pozzolanic reaction of GGBS, which breaks down calcium hydroxide to create more C-S-H gel, is what causes this reduction. The concrete's stability and durability are improved by the finer microstructure that results from this reaction, which increases its resistance to heat fluctuations and chemical attacks.

Trace elements such as magnesium and potassium are also noted by XRD analysis. Though present in smaller amounts, these elements play an important role in the regulation of concrete performance. Magnesium contributes to the stabilization of hydration products, whereas potassium influences the setting time and chemical stability of the material. These elements improve the durability of the concrete through enhanced resistance to chemical reactions and environmental degradation [24-25].

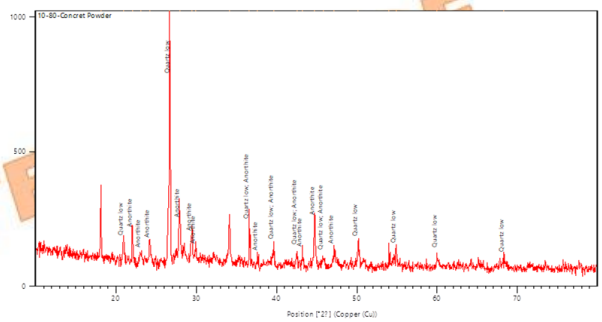

Fig. 11. XRD analysis of concrete mix with GGBS and NS

3.7. Scanning Electron Microscopy (SEM)

The SEM of concrete containing GGBS and NS, presented in Figure 12, clearly brings out the improvements achieved by these supplementary materials on microstructural levels. GGBS particles, from SEM images, have irregular shapes, are angular, and have a rough surface that is rough, hence greatly increasing their reactivity.

Angular morphology of GGBS is beneficial for accelerating hydration reactions as well as for interlocking within the concrete matrix. Improved early-age strength and a densified microstructure result from the rapid formation of the C-S-H gel during the initial stages of hydration, which is one characteristic of this increased reactivity.

Nano-Silica, however, demonstrates a spherical morphology with very small particle sizes and hence an ultra-high surface area. These features enable NS to fill voids within the cementitious matrix, which effectively refines the microstructure with concomitant reduction of permeability. The high surface area of NS enhances nucleation of hydration products and ensures the distribution of C-S-H gel is more uniform. The interfacial transition zone, which in turn is sandwiched between the aggregates and the cement paste, will thus undergo densification and, with that, result in the minimization of the microcracking and overall durability increase in the concrete. Secondly, NS will accelerate hydration of tricalcium silicate C3S, thus enhancing the compression and tensile strength since a refined compact C-S-H gel results directly.

The SEM analysis also points toward a synergistic effect while using GGBS along with NS. The coarse surfaces of GGBS particles serve as nucleation sites for the hydration products of Nano-Silica, thus further enhancing the density and homogeneity of the matrix. Such a synergy results in an increased interconnectivity and stability of the microstructure and enhances both the mechanical and durability properties of the concrete. These indicate the reduction in porosity and improved distribution of the hydration products, which appear quite prominent in the SEM micrographs, thus corroborating the positive interaction of GGBS with NS.

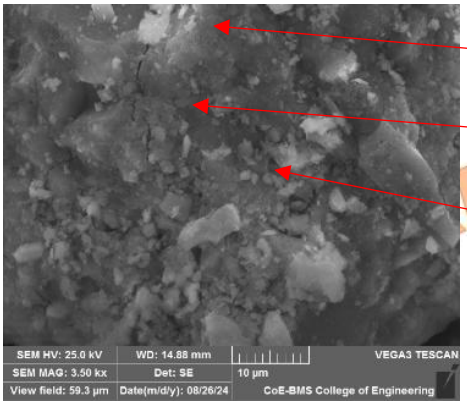

(a) Conventional Concrete

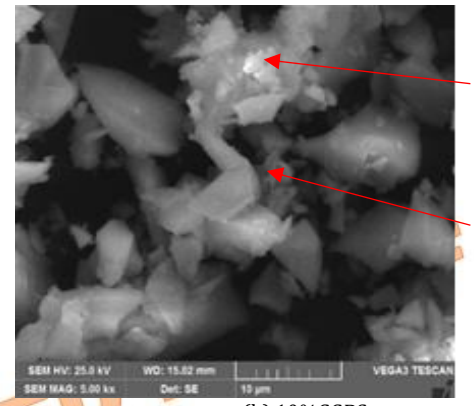

(b) 10%GGBS

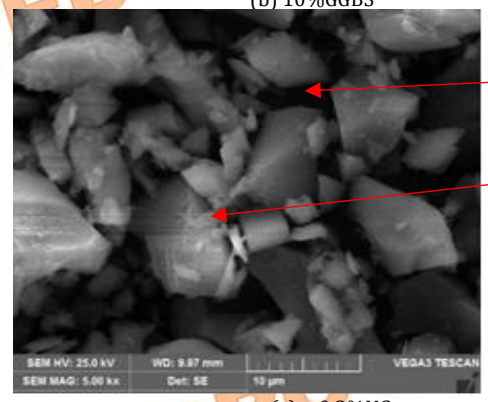

(c) 0.3%NS

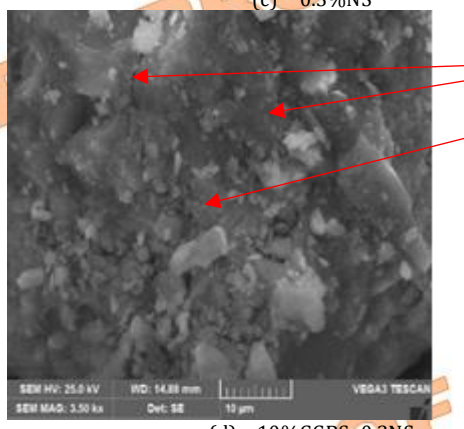

(d) 10%GGBS+0.3NS

Figure 12: SEM of different samples

From microstructure analysis, it can be noted that improved strength characteristics are due to increased packing density of angular particles of GGBS and NS and formation of C-S-H. The observations made in the current study are in line with and in good agreement with previous studies. Siddique and Rajor [20] proved that GGBS enhanced the tensile strength of concrete by microstructural refinement along with low permeability. Singh et al. [21] showed that the addition of Nano-Silica enhances early-age properties along with overall tensile strength through its filler effect and hydration acceleration. Ramezanianpour et al. [22] pointed out the beneficial effects of GGBS blended with NS. These observations illustrate that the optimized dosages could significantly enhance

both the compressive and tensile strength properties.

3.8. Failure Pattern

The failure pattern of the control slab, as shown in Figure 13a, follows the principles of yield line theory. Under loading, plastic hinges formed at critical sections, resulting in a characteristic failure shape. Observations indicate that the steel reinforcement reached its yield strength before the concrete experienced significant fracture, suggesting the slab was under-reinforced. This mode of failure is advantageous in design because it promotes ductile behavior, providing a clear warning prior to complete failure. The slab exhibited a gradual failure pattern, demonstrating the ductility imparted by the reinforcing steel and significant energy absorption during deformation. Figure 13b illustrates the failure pattern of slabs incorporating GGBS and Nano-Silica. Similar to the control slab, plastic hinges formed in line with yield line theory. However, the inclusion of these supplementary materials delayed crack initiation and improved stress distribution across the slab, likely due to a denser microstructure and enhanced interfacial transition zone (ITZ). The slab displayed gradual failure with higher energy absorption, increased load-bearing capacity, and improved ductility, making it both stronger and safer. This behavior highlights the effectiveness of GGBS and Nano-Silica in enhancing resilience and ductile performance in reinforced concrete slabs.

Fig. 13. Failure pattern of the slab

4. Conclusions

1. The addition of mineral admixtures in concrete resulted in increased density, mechanical strength, and decreased porosity.

2. The optimum combination of GGBS and NS was 10% and 0.3%, respectively, resulting in strength enhancement by 18.26 and 23.68%, respectively. Use of a combination og GGBS and NS resulted in mechanical properties by 11%.

3. Slab specimens prepared with an optimum dosage of GGBS and NS exhibited an improvement of 15% in ductility index as compared to control specimens, indicating improved deformation capacity and energy absorption before failure.

4. Thinner slabs (for example, 80 mm) containing GGBS and NS exhibited 34.5% greater strength than conventional 100 mm thick slabs.

5. Variation in the size of aggregates to 12.5–10 mm increases stiffness in slabs. Around 12% improvement in stiffness was observed for slabs.

These outcomes validate that the application of GGBS and Nano-Silica improves the strength and ductility of concrete and also delivers efficient and sustainable construction solutions. Also, variations in mix design and strength levels may further affect the mechanical properties, ductility, and energy absorption capacity of the slabs.

Limitations and Scope for Future Work

As mentioned in the manuscript, this study provides a simple mixing approach using a drum mixer. Further, the outcome of this study can be compared with a cementitious matrix prepared by varying the blending duration.

Acknowledgments

We would like to thank UBDT College for providing the basic support.

Funding Statement

This research work is not funded by any organization

Conflicts of Interest

The authors declare that there is no conflict of interest regarding the publication of this article.

Data Availability

The data used to support the findings of this study are included within the article. Further data or information is available from the corresponding author upon request.

References

[1] O. Zaid, F. M. Mukhtar, R. M-García, M. G. El Sherbiny, and A. M. Mohamed, "Characteristics of high-performance steel fiber reinforced recycled aggregate concrete utilizing mineral filler," Case Studies in Construction Materials, vol. 16, Jun. 2022, doi: 10.1016/j.cscm.2022.e00939.

[2] O. Zaid, S. R. Z. Hashmi, F. Aslam, Z. U. Abedin, and A. Ullah, "Experimental study on the properties improvement of hybrid graphene oxide fiber-reinforced composite concrete," Diam Relat Mater, vol. 124, Apr. 2022, doi: 10.1016/j.diamond.2022.108883.

[3] O. Zaid, J. Ahmad, M. S. Siddique, F. Aslam, H. Alabduljabbar, and K. M. Khedher, "A step towards sustainable glass fiber reinforced concrete utilizing silica fume and waste coconut shell aggregate," Sci Rep, vol. 11, no. 1, Dec. 2021, doi: 10.1038/s41598-021-92228-6.

[4] S. Tangaramvong, P. Nuaklong, M. T. Khine, and P. Jongvivatsakul, "The influences of granite industry waste on concrete properties with different strength grades," Case Studies in Construction Materials, vol. 15, Dec. 2021, doi: 10.1016/j.cscm.2021.e00669.

[5] F. Althoey et al., "Impact of sulfate activation of rice husk ash on the performance of high strength steel fiber reinforced recycled aggregate concrete," Journal of Building Engineering, vol. 54, Aug. 2022, doi: 10.1016/j.jobe.2022.104610.

[6] J. Mishra, B. Nanda, S. K. Patro, and R. S. Krishna, "A comprehensive review on compressive strength and microstructure properties of GGBS-based geopolymer binder systems," Feb. 23, 2024, Elsevier Ltd. doi: 10.1016/j.conbuildmat.2024.135242.

[7] F. Kanavaris, M. Soutsos, and J. F. Chen, "Enabling sustainable rapid construction with high volume GGBS concrete through elevated temperature curing and maturity testing," Journal of Building Engineering, vol. 63, Jan. 2023, doi: 10.1016/j.jobe.2022.105434.

[8] H. Singh, A. Kumar Tiwary, and S. Singh, "Experimental investigation on the performance of ground granulated blast furnace slag and nano-silica blended concrete exposed to elevated temperature," Constr Build Mater, vol. 394, Aug. 2023, doi: 10.1016/j.conbuildmat.2023.132088.

[9] P. S. Deb, P. Nath, and P. K. Sarker, "The effects of ground granulated blast-furnace slag blending with fly ash and activator content on the workability and strength properties of geopolymer concrete cured at ambient temperature," Mater Des, vol. 62, pp. 32–39, 2014, doi: 10.1016/j.matdes.2014.05.001.

[10] O. Afzali Naniz and M. Mazloom, "Effects of colloidal nano-silica on fresh and hardened properties of self-compacting lightweight concrete," Journal of Building Engineering, vol. 20, pp. 400–410, Nov. 2018, doi: 10.1016/j.jobe.2018.08.014.

[11] Saravanan, D., et al. "Tribological properties of filler and green filler reinforced polymer composites." Materials Today: Proceedings 50 (2022): 2065-2072. https://doi.org/10.1016/j.matpr.2021.09.414.

[12] O. Zaid, J. Ahmad, M. S. Siddique, and F. Aslam, "Effect of Incorporation of Rice Husk Ash Instead of Cement on the Performance of Steel Fibers Reinforced Concrete," Front Mater, vol. 8, Jun. 2021, doi: 10.3389/fmats.2021.665625.

[13] L. A. Qureshi, B. Ali, and A. Ali, "Combined effects of supplementary cementitious materials (silica fume, GGBS, fly ash and rice husk ash) and steel fiber on the hardened properties of recycled aggregate concrete," Constr Build Mater, vol. 263, Dec. 2020, doi: 10.1016/j.conbuildmat.2020.120636.

[14] S. K. Rao, P. Sravana, and T. C. Rao, "Abrasion resistance and mechanical properties of Roller Compacted Concrete with GGBS," Constr Build Mater, vol. 114, pp. 925–933, Jul. 2016, doi: 10.1016/j.conbuildmat.2016.04.004.

[15] V. Jayanthi et al., "Innovative use of micronized biomass silica-GGBS as agro-industrial by-products for the production of a sustainable high-strength geopolymer concrete," Case Studies in Construction Materials, vol. 18, Jul. 2023, doi: 10.1016/j.cscm.2022.e01782.

[16] Gopalakrishnan, V., & Somasundaram, S. (2018). Effect of GGBS on compressive strength of concrete. Materials Today: Proceedings, 5(2), 6850–6857.

[17] Vinod, M., Kumar, C.A., Sollapur, S.B. et al. Study on Fabrication and Mechanical

Performance of Flax Fibre-Reinforced Aluminium 6082 Laminates. J. Inst. Eng. India Ser. D (2023). https://doi.org/10.1007/s40033-023-00605-4.

[18] Singh, L. P., & Siddique, R. (2016). Effect of nano-silica on properties of concrete. Construction and Building Materials, 119, 71–82.

[19] Torkittikul, P., & Chaipanich, A. (2020). Role of nano-silica in concrete performance. Cement and Concrete Composites, 109, 103564.

[20] Siddique, R., & Rajor, A. (2017). Strength and durability properties of concrete incorporating GGBS. Construction and Building Materials, 144, 234–247.

[21] Singh, L. P., Karade, S. R., & Elchalakani, M. (2018). Role of nano-silica on the tensile properties of concrete. Materials and Structures, 51(4), 92–105.

[22] Vinod, M., Kumar, C.A., Sollapur, S.B. et al. Study on Low-Velocity Impact Performance of Chemical Treated Flax Fibre-Reinforced Aluminium 6082 Laminates. J. Inst. Eng. India Ser. D (2024). https://doi.org/10.1007/s40033-024-00657-0

[23] Ramezanianpour, A. A., Mahdikhani, M., & Ahmadibeni, G. (2015). The effect of GGBS and nano-silica on the properties of concrete. Cement and Concrete Composites, 40, 106–114.

[24] Venkate Gowda, C., Nagaraja, T.K., Yogesha, K.B. et al. Study on Structural Behavior of HVOF-Sprayed NiCr/Mo Coating. J. Inst. Eng. India Ser. D (2024). https://doi.org/10.1007/s40033-024-00641-8

[25] Neville, A. M. (2011). Properties of Concrete (5th ed.). Pearson Education.

[26]Asadi Jafari, M. H., Zarastvand, M., & Zhou, J. (2024). Doubly curved truss core composite shell system for broadband diffuse acoustic insulation. Journal of Vibration and Control, 30(17-18), 4035-4051.

[27]Abdoli, E., Zarastvand, M. R., & Talebitooti, R. (2025). Wave propagation numerical simulation approach based on a novel TPMS-based lattice metamaterial for improved vibration transmission of doubly curved sandwich systems. Engineering with Computers, 1-18.

[28] Talebitooti, R., & Zarastvand, M. R. (2018). Vibroacoustic behavior of orthotropic aerospace composite structure in the subsonic flow considering the Third order Shear Deformation Theory. Aerospace Science and Technology, 75, 227-236.

[29]Shabrou, M., & Daneshjoo, Z. (2025). Development of generalized mixed-mode I/II fracture criteria for arbitrary cracked orthotropic materials considering fracture process zone. Archive of Applied Mechanics, 95(5), 114.

[30] Fakoor, M., Ghodsi, S., Izadi, S. M. H., & Daneshjoo, Z. (2025). Exploring Fracture Toughness in the Damage Zone of Fiber-Reinforced Composites: A Study on Crack Orientation Effects. Arabian Journal for Science and Engineering, 1-10.

[31]Shirzadeh, Z., Fakoor, M., & Daneshjoo, Z. (2025). Simulating delamination in composite laminates with fracture process zone effects: A novel cohesive zone modeling approach. Engineering Fracture Mechanics, 315, 110834.

[32] Daneshjoo, Z., & Bazzazian, H. (2024). An extended multi-linear cohesive zone model for mixed-mode I/II delamination growth simulation in composite laminates with R-curve effects. Archive of Applied Mechanics, 94(10), 2793-2805.

[33] Aydın, F., Boru, E., Durmaz, N., Sarıbıyık, A., Sarıbıyık, M., & Aydın, E. (2024). An Experimental Investigation of Flexural Performance of FRP Reinforced Concrete Slabs. International Journal of Civil Engineering, 22(12), 2269-2282.